Isothermal Growth of Low Molecular Weight Polyethylene Single Crystals from Solution. 2. Melting and Dissolution Behavior

W. M. Leung and R. St. John Manley*

Pulp and Paper Research Institute of Canada and Department of Chemistry, McGill University, Montreal, Quebec, Canada H3A 2A7

A. R. Panaras

Societé National Elf Aquitaine (Production), Centre de Recherches de Lacq, B.P. 34, 64170 Artix, France. *Received August 31, 1983*

ABSTRACT: Melting and dissolution temperatures (T_m and T_d) and enthalpies of fusion (ΔH) have been measured as a function of crystallization temperature (T_c) for solution-grown crystals of polyethylene fractions covering the molecular weight range 1000–11 600. Analysis of the data yields values of the basal surface free energies σ_e which increase with molecular weight and lie in the range 40–60 erg/cm^2 for the molecular weights from 3100 to 11 600. Values of the equilibrium melting/dissolution temperatures obtained from the intercept of T_m (T_d) plots vs. the reciprocal lamellar thickness are in good agreement with those obtained from direct measurements on extended-chain crystals of large lateral dimensions and thickness. The enthalpies of fusion of the crystals of the various fractions generally increase monotonically with T_c in parallel with their thickness. However, for samples with molecular weights of 3100 and 4050 sigmoidal curves are obtained when the enthalpies of fusion are plotted against crystallization temperature. This is interpreted to mean that in this molecular weight range there is a transition in the number of folds per molecule deposited on the growth faces as T_c increases.

Introduction

The problem of chain folding in polymers has attracted much interest since the discovery of the phenomenon some 25 years ago.[1,2] Despite the considerable advances that have been achieved a complete understanding of the mechanism remains a challenge. As stated in part 1, the basic aim of the present work is to study the growth kinetics and physical properties of solution-grown crystals of low molecular weight polyethylene fractions for which the transition from extended-chain to folded-chain growth can be observed. The first phase of the investigation, described in part 1, involved the measurement of the variation of the lamellar thickness of the crystals with the temperature of crystallization T_c and of the equilibrium dissolution temperature of the samples with molecular weight. It was found that the lamellar thickness increases monotonically with crystallization temperature, which indicates that the chains undergo a gradual unfolding as the supercooling decreases. This behavior may be contrasted with that of low molecular weight poly(ethylene oxide) single crystals grown from the melt for which the lamellar thickness increases in a stepwise manner with T_c.[3-5]

The immediate purpose of the present paper is to further characterize the low molecular weight polyethylene crystals by examining their thermal behavior through differential scanning calorimetry (DSC). The pattern of the paper is as follows. First we consider the effect of the heating rate on the melting/dissolution temperature of crystals grown from solution at various temperatures. By analysis of the DSC curves the melting and dissolution temperatures of the crystals are obtained. The next stage in the paper involves the analysis of melting point (T_m)/dissolution temperature (T_d) and crystal thickness (l) measurements in order to estimate values of the basal surface free energies and the equilibrium melting/dissolution temperatures.

Finally, measurements are presented of the enthalpy of fusion of the low molecular weight polyethylene crystals grown at various temperatures. From these data information on the structure of the basal crystal surfaces is derived. The principal finding of these studies is that crystals in the molecular weight range of 3000–4000 exhibit a transition in the conformation of the molecules (i.e., the number of folds per molecule) deposited on the growth faces as the crystallization temperature is increased.

Experimental Section

The samples used were linear polyethylenes covering the molecular weight range from 1000 to 11 600. Details of the origin and characterization of the samples have been given in Table I in part 1. The solvent used was commercial *p*-xylene distilled before use.

Crystallization from dilute xylene solutions was carried out isothermally over a temperature range 35–65 °C for PE1000 and 65–90 °C for the other fractions. The procedure used was similar to that described by Holland and Lindenmayer.[6] A solution of the polymer in xylene was prepared at 110 °C. A suitable aliquot of this solution was added with gentle stirring to an appropriate amount of pure xylene which had previously been brought to the crystallization temperature. In this way the time required to establish thermal equilibrium was minimized and the stirring was discontinued. The final concentration at which the crystals grew was in the range 0.02–0.5% (w/w) depending on the supercooling. The suspension of crystals was filtered at the crystallization temperature, washed first with aliquots and fresh xylene and then with acetone, and dried in vacuo at room temperature.

Thermal measurements of the different fractions were performed in a Perkin-Elmer differential scanning calorimeter, Model DSC-2C. For the measurement of melting and dissolution temperatures, approximately 0.1 mg of the dry sample was weighed into sealable sample pans by using a Cahn electrobalance. When dissolution temperatures were to be measured, an aliquot of xylene was delivered to the sample pan by microsyringe, and the sample pan was then hermetically sealed and weighed to determine the amount of solvent. The concentrations were in the range 0.4–0.5% (w/w). It has been demonstrated in part 1 that the dissolution temperature measured by DSC is essentially independent of concentration within this concentration range.

The apparent melting/dissolution temperature was determined from the peak temperature of the endotherms. It is well-known that polymer crystals tend to thicken during heating and rapid heating rates have often been used to minimize this effect.[7] In the present work the samples were heated at different rates up to 160 °C/min; the apparent melting/dissolution temperatures were plotted against heating rate and extrapolated to zero heating rate to obtain the true melting/dissolution temperature.

The temperature scale of the calorimeter was calibrated with naphthalene (T_m = 80.2 °C), benzoic acid (T_m = 122.4 °C), and indium (T_m = 156 °C). Standard corrections were made for changes in melting temperature and thermal resistance as a function of heating rate.[8]

The heats of fusion of the dry crystals were determined from the area under the melting endotherm. For these measurements

0024-9297/85/2218-0753$01.50/0

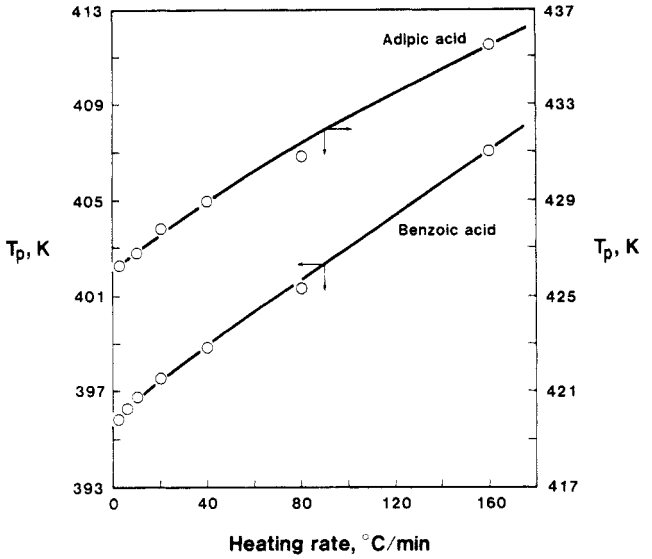

Figure 1. Melting peak temperatures T_p as a function of heating rate s for adipic and benzoic acid.

the sample sizes were in the range of 0.2–0.3 mg. The DSC base line was stored in the calorimeter computer and was subtracted from subsequent runs. The value of the heat of fusion was calibrated with indium heated under the same running conditions. Heating rates of 5–20 °C/min were found to have no effect on the value of the heat of fusion. At least four runs were made for each sample and averaged to obtain the heat of fusion. The precision of the results from these repeated experiments was ±1 cal/g.

Results and Discussion

Melting and Dissolution Behavior. When simple substances such as benzoic acid are heated in the DSC, only a single melting peak is observed. Moreover, the melting peak temperature T_p increases monotonically with heating rate, s. This is illustrated in Figure 1 for benzoic and adipic acids. The continuous increase in T_p with heating rate has been explained as due to the thermal inertia of the sample[9] and possibly the finite melting rate of the crystals.[10,11] The true melting temperature T_m can be obtained by extrapolating the curve to zero heating rate.

When the melting peak temperature of the dry polyethylene single crystals is plotted against heating rate, the results are quite different from those of simple substances. As shown in Figure 2 for the single crystals of the fractions PE11600 and PE6750 the fusion curves usually show two melting peaks at low heating rates (i.e., below s = 20). At higher heating rates the two peaks broaden and merge to a single peak. For the first (low-temperature) peak T_p remains in the same position as s increases. On the other hand, for the second (high-temperature) peak T_p first decreases with heating rate, and then after passing through a minimum it increases monotonically with heating rate (Figure 3). These features are very similar to those shown by poly(ethylene oxide), as analyzed by Buckley and Kovacs,[20] and can be interpreted in terms of partial melting followed by recyrstallization. Thus, the peak at the lower temperature represents the partial melting of the initially present crystals, while the upper peak corresponds to the complete melting of recrystallized or reorganized material. Accordingly, for these samples the true melting temperature can be obtained by extrapolating the apparent melting point of the first peak to zero heating rate. As mentioned above, for the second peak T_p passes through a minimum and then increases with s in the manner characteristic of simple substances. Experimental results show that the extrapolated value of the second melting peak T_p at s = 0 is within the experimental error equal to T_p of the first peak. This suggests that at sufficiently high heating rates the origin of the second peak changes. No longer does it represent the melting of recrystallized material; rather, since the crystals are unable to reorganize in the time scale of the experiment, it corresponds to zero entropy production melting[12] of the original material at the particular

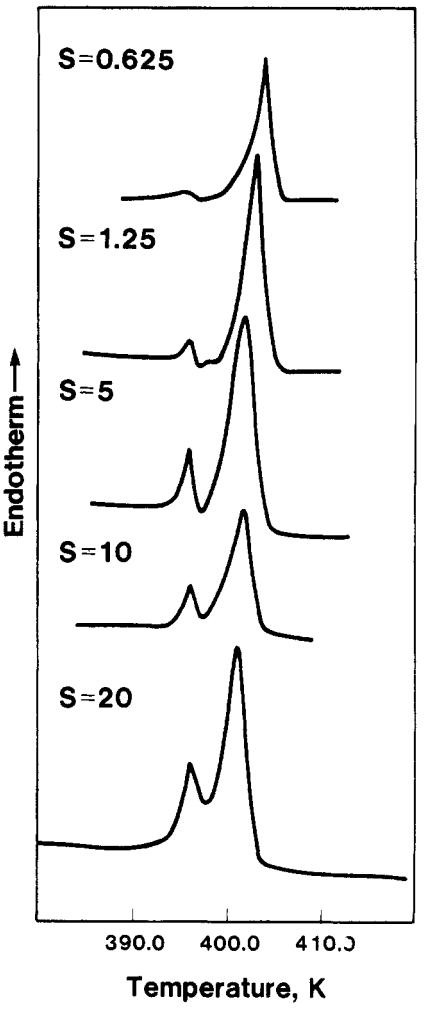

Figure 2. Melting endotherms obtained at different heating rates s (in °C/min) for fraction PE6750 crystal aggregates grown at 84.5 °C from xylene solution.

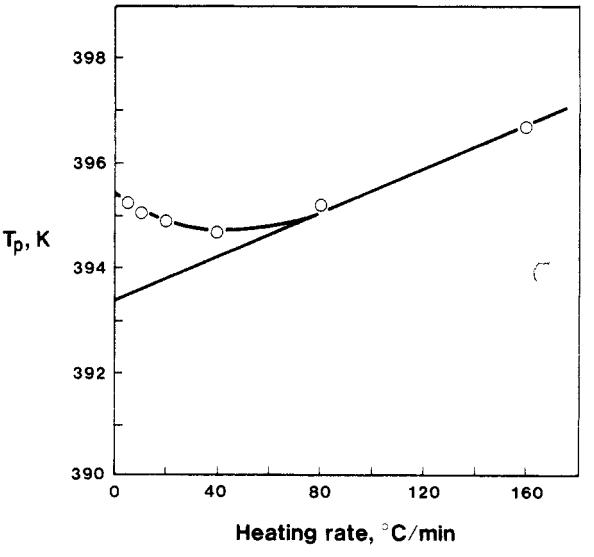

Figure 3. Melting peak temperatures T_p vs. heating rate s for sample PE6750 crystallized from xylene at 74 °C.

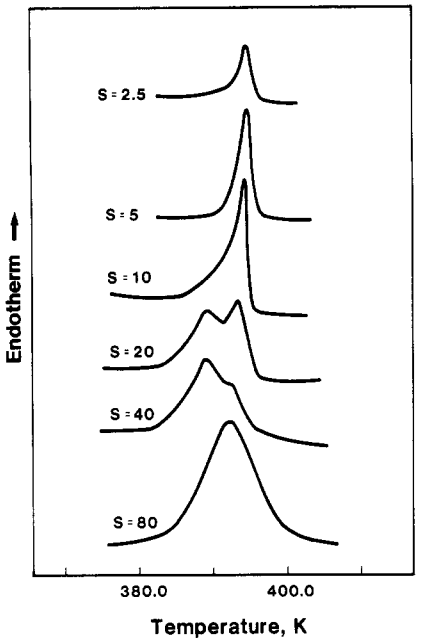

Figure 4. Melting endotherms obtained at various heating rates s (°C/min) for PE3100 crystals grown from xylene at 74.5 °C.

heating rate. Accordingly it may be assumed that extrapolation of T_p of the second peak from higher s values to $s = 0$ gives the true melting point of these fractions. Due to the long extrapolation the error in estimating T_m in this way is about ±1 °C.

Let us now consider the fractions PE3100 and PE4050. As an example, Figure 4 shows typical endotherms for PE3100 crystallized at temperatures in the range of 60–75 °C. At the lower heating rates of 2.5–10 °C/min, only a single endotherm peak is observed and this is assigned to the melting of reorganized or recrystallized material. This may be compared with the behavior of the higher molecular weight fractions for which two peaks appear even at heating rates as low as 0.625 °C/min. Clearly reorganization in these samples is much more rapid than in the previous examples. This is not surprising since, as will be seen later, PE3100 and PE4050 are composed only of extended, once- or twice-folded chains depending on the crystallization temperature. As the heating rate increases, two peaks appear corresponding to partial melting of the original crystals (lower peak) and complete melting of recrystallized material (upper peak). Finally, at the highest heating rates ($s > 80$ °C/min) a single endotherm peak is again observed because sufficient time is not available for reorganization. This single high-temperature peak thus represents zero entropy production melting of the original crystals. By plotting T_p of the high-temperature peak against s, we used the extrapolation procedure described above to obtain the true melting point of these samples (Figure 5).

Finally, for the fractions PE1000 and PE2000 the DSC curves show only one endotherm peak at all heating rates. This is consistent with the fact that these crystals are essentially extended-chain structures and therefore less susceptible to reorganization than the higher molecular weight samples. As shown in Figure 6, the melting peak temperatures are almost independent of s at the lowest heating rates, but at higher heating rates T_p increases with s as for simple substances. Thus, the true melting point could be obtained by the extrapolation procedure described before.

Figure 7 shows an example of the DSC curves obtained when the crystals of the various fractions were heated in

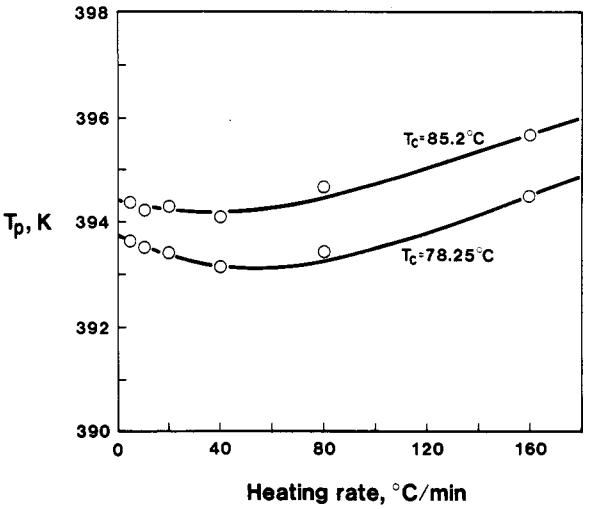

Figure 5. Melting peak temperature T_p as a function of heating rate s for crystals of PE4050 grown from xylene at two different temperatures.

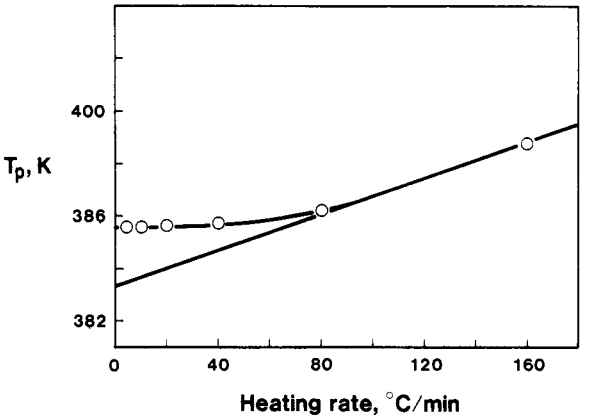

Figure 6. Melting peak temperature T_p as a function of heating rate s for crystals of PE2000 grown in xylene at 65 °C.

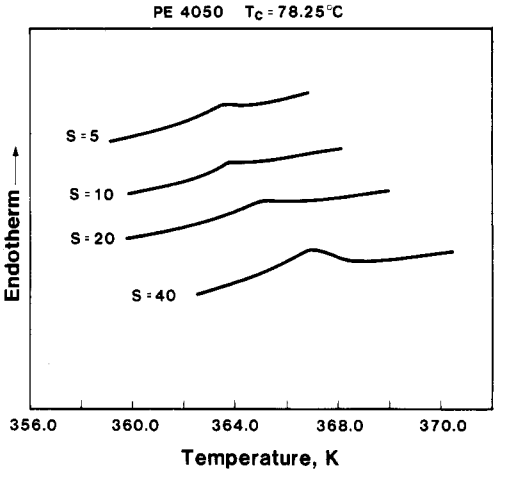

Figure 7. Melting endotherms obtained at various heating rates s (°C/min) for PE4050 crystals (T_c = 78.2 °C) in the presence of xylene.

the presence of solvent. In all cases only a single endotherm peak is observed. The principal effect of the solvent is to cause a lowering of the melting temperature. As illustrated in Figure 8, the endotherm peak temperature increases continuously with s. This indicates that there is little or no rearrangement or annealing in the crystals before dissolution. This observation is in agreement with the results obtained by Blackadder and Schleinitz[13] which show that heating rates of 1–2 °C/min are high enough

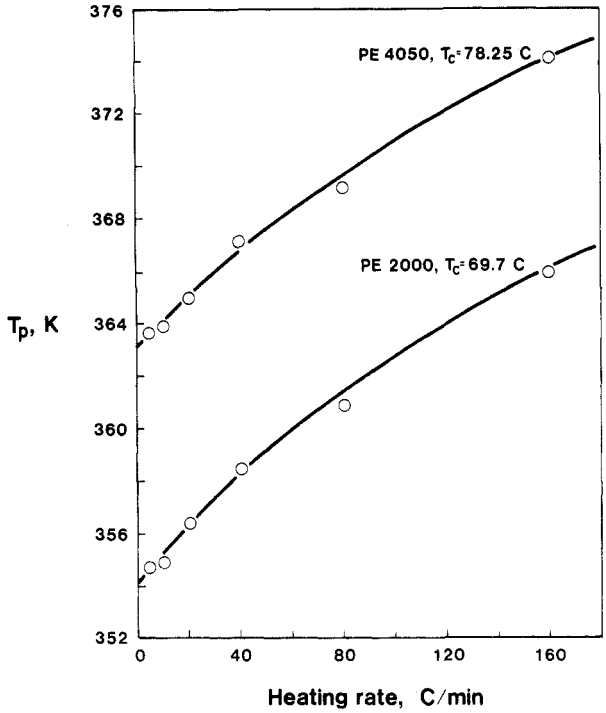

Figure 8. Melting peak temperatures T_p in the presence of xylene vs. heating rate s for crystals of PE2000 and PE4050.

to suppress the annealing of crystals in the presence of solvent. Extrapolation of the curve to $s = 0$ gives the true dissolution temperature.

The various values of T_m and T_d obtained from the fusion and dissolution studies are summarized in Table I. As expected, the values of T_m and T_d increase with T_c in parallel with the thickness of the crystals.

Surface Free Energies and Equilibrium Melting/Dissolution Temperatures. A widely used method for determining the basal surface free energy σ_e and the equilibrium melting temperature T_m° of polymer crystals is based upon the relation (the so-called Gibbs–Thompson equation) first applied to polymers by Hoffman and Weeks[14]

$$T_m = T_m^\circ\left[1 - \frac{2\sigma_e}{\Delta h_f}\frac{1}{l}\right] \quad (1)$$

where Δh_f is the heat of fusion per unit volume of the crystal, T_m is the observed melting point of the crystal, and l is the crystal thickness. Accordingly a plot of T_m against $1/l$ should be linear with a slope of $2\sigma_e T_m^\circ/\Delta h_f$ and an intercept of T_m°. Thus, if Δh_f is known, σ_e can be determined. In the case of dissolution experiments T_m° in eq 1 is replaced by T_d°, the equilibrium dissolution temperature. For high molecular weight polyethylene samples[15,16] eq 1 is obeyed within the experimental error and a value of $\sigma_e = 93 \pm 8$ erg/cm^2 is obtained for both dried single crystals and single crystals in xylene suspensions. The value of T_m° is about 146 °C for dried single crystals and the equilibrium dissolution temperature T_d° is 114 °C (xylene). Bair and Salovey[17] have shown that σ_e is approximately independent of molecular weight in the moderate to high range. However, it is known that for low molecular weight samples, σ_e depends upon the chain length and increases to the asymptotic value of about 93 erg/cm^2 at high molecular weights.[18,19]

For the various fractions studied in the present work the data compiled in Table I were plotted in accordance with eq 1. Examples are shown in Figures 9 and 10. Linear relations were obtained for all but the two lowest fractions.

Table I
Melting/Dissolution Temperatures and the Reciprocal of the Lamellar Thickness of Polyethylene Single Crystals Grown at Various Temperatures T_c[a]

T_c, K	T_m, K	T_d, K	$10^3(1/l)$, Å^{-1}
	PE11600		
341.5	397.7	369.2	9.37
347.2	398.4	369.4	8.85
354.1	400.9	372.1	7.94
358.1	401.3	372.5	7.25
365.8	405.7	375.6	5.00
	PE6750		
333.3	391.7	364.5	9.80
341.5	391.9	365.6	9.37
347.2	393.4	366.1	8.85
354.1	394.4	366.6	7.97
357.7	395.5	366.7	7.35
363.1	396.5	369.8	6.06
	PE4050		
333.3	388.5	360.2	9.26
341.2	389.9	361.5	8.55
347.2	390.1	361.8	7.75
351.4	391.6	363.1	7.25
353.4	392.4	363.4	6.58
358.4	393.4	364.1	6.04
	PE3100		
333.3	386.8	355.4	8.97
341.2	387.6	356.9	8.03
347.7	388.5	357.3	7.09
353.2	390.4	359.2	6.21
357.5	391.0	359.5	5.24
	PE2000		
333.7	382.6	351.0	9.08
338.2	383.5	352.0	8.13
342.9	384.0	354.1	7.25
348.2	386.1	354.4	6.49
353.4	386.5	359.6	6.15
	PE1000		
309.5	380.4	339.8	10.15
324.4	381.3	341.1	9.39
332.1	383.1	342.9	8.70
337.8	383.4	345.9	8.51

[a] Lamellar thickness data have already been presented in part 1.

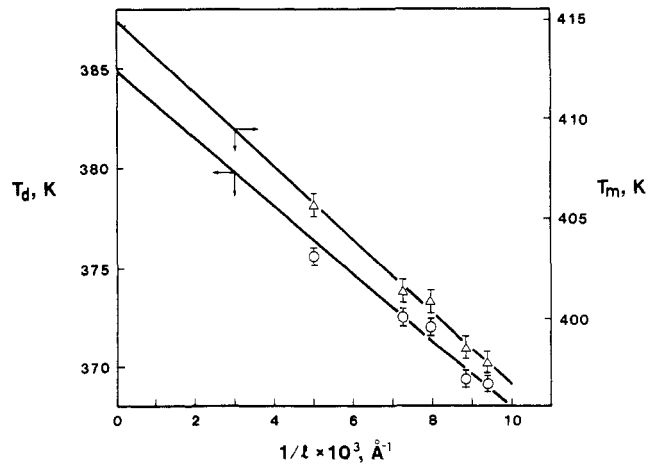

Figure 9. Melting (T_m) and dissolution (T_d) temperatures as a function of reciprocal lamellar thickness for PE11600 crystals.

Adopting $\Delta h_f = 2.8 \times 10^9$ erg/cm^3, we have collected in Table II values of σ_e, T_m°, and T_d° obtained from the plots. Also included in the table are values of σ_e obtained from the analysis of measurements of lamellar thickness as a function of supercooling as described in part 1. It is seen that within the experimental error the values of σ_e obtained by the two methods are in good agreement but they are

Table II
Basal Surface Free Energy σ_e and the Equilibrium Melting/Dissolution Temperatures ($T_m°/T_d°$) Obtained from a Plot of T_m (or T_d) vs. $1/l$

	σ_e, erg/cm^2			$T_m°$, K		$T_d°$, K	
fraction	from T_m data	from T_d data	av	from part 1[a]	from eq 1	from part 1[b]	from eq 1	from part 1[c]
PE11600	62.8	60.7	61.7	60.1	415.0	412.7	384.8	382.0
PE6750	49.1	48.7	48.9	51.7	406.8	410.1	377.7	376.8
PE4050	45.3	45.6	45.5	48.5	401.8	406.8	372.0	371.5
PE3100	42.2	40.7	41.5	48.9	398.2	403.7	365.7	367.4

[a] From the analysis of lamellar thickness as a function of supercooling. [b] From direct calorimetric measurements on macroscopic extended-chain crystals. [c] From direct calorimetric measurements on macroscopic extended-chain crystals in the presence of solvent.

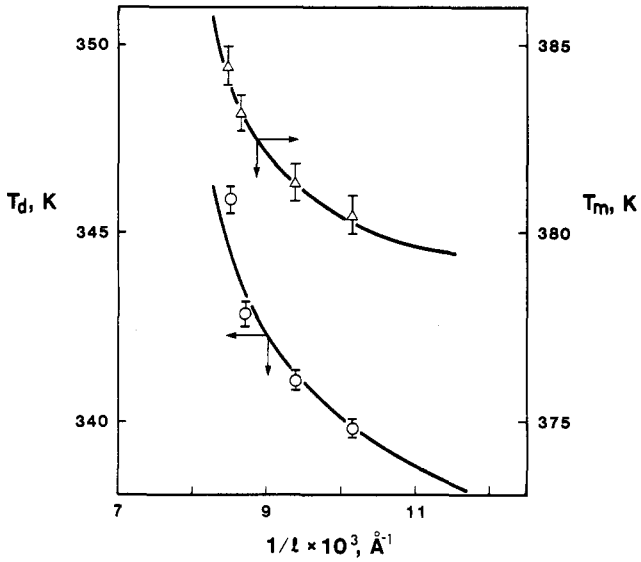

Figure 10. Melting (T_m) and dissolution (T_d) temperatures as a function of reciprocal lamellar thickness for crystals of PE1000.

considerably lower than the accepted value of 93 erg/cm^2 obtained for high molecular weight samples. The difference is probably caused by the inclusion of chain-end effects in the effective value of σ_e due to the finite chain length of the samples. It may also be noted that σ_e increases with molecular weight over the range encompassed. This behavior is expected for these low molecular weight samples since chain-end effects will diminish with increasing molecular weight; furthermore, it implies that as the molecular weight increases there are significant differences in the structure of the surface layers of the lamellae.

Turning now to the results for the equilibrium melting and dissolution temperatures, we can see from Table II that the values derived from eq 1 are in reasonably good accord with the directly measured values using extended-chain crystals of each fraction as described in part 1. It should be emphasized that in the present work the values of the equilibrium melting and dissolution temperatures obtained from eq 1 relate to extended-chain crystals of large lateral dimensions and thickness corresponding to a finite number of chain units. It is therefore not surprising that the values are lower than the equilibrium melting/dissolution temperatures for polyethylene crystals with chains of infinite length ($T_m°$ = 419 K; $T_d°$ = 387 K) as cited above.

Buckley and Kovacs[20] have shown that eq 1 has limitations when applied to low molecular weight polymers. Nevertheless, this is not apparent in the present work with polyethylene fractions having molecular weights in the range of 3100–11 600. In fact the good agreement between the σ_e values derived from eq 1 and those obtained from the $l(1/\Delta T)$ curves indicates that theory and experiment are consistent. Therefore, we can proceed with confidence to use these σ_e values as a standard from which to assess the significance of the σ_e values obtained from growth rate data to be presented in part 3.

Table III
Enthalpy of the Fusion of the Polyethylene Single Crystals

T_c, °C	ΔH, cal/g	T_c, °C	ΔH, cal/g
PE11600		PE6750	
68.3	52.8	68.3	53.6
74.0	53.5	74.0	56.0
80.9	56.7	80.9	57.0
84.9	58.0	84.5	58.1
92.6	60.4	89.9	59.9
PE4050		PE3100	
60.1	54.8	60.1	54.3
68.0	55.4	68.0	55.5
70.0	56.4	69.8	56.6
74.0	55.9	74.0	58.5
78.2	59.1	83.2	64.7
82.2	63.7	86.9	65.7
85.2	64.7		
PE2000		PE1000	
60.5	63.5	36.3	63.0
65.0	64.4	51.2	64.2
70.4	64.9	58.9	64.7
75.0	65.4	64.6	64.9
80.2	65.7		

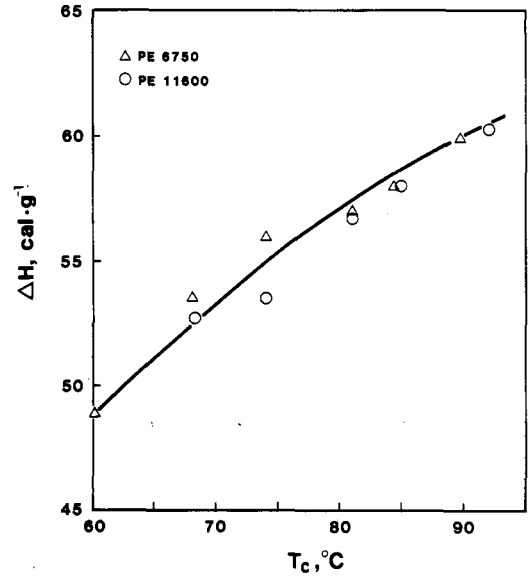

Figure 11. Plots of the enthalpy of fusion ΔH vs. crystallization temperature T_c for fractions PE6750 and PE11600 crystallized from xylene solution.

Enthalpies of Fusion. Table III lists the results for the measurement of the enthalpy of fusion of the various fractions crystallized isothermally from solution at different temperatures and filtered at the crystallization temperature. In Figures 11 and 12 the enthalpies of fusion ΔH are plotted against crystallization temperature. For PE11600 and PE6750 (Figure 11) the results fall on a common curve that increases monotonically with tem-

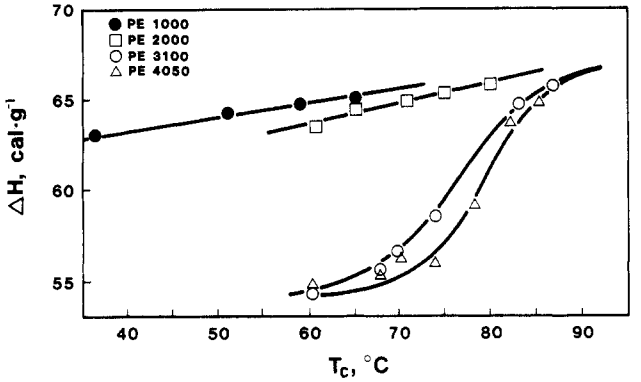

Figure 12. Plots of the enthalpy of fusion ΔH vs. crystallization temperature T_c for fractions PE1000, PE2000, PE3100, and PE4050 crystallized from xylene solution.

perature in the range investigated. Similar behavior is observed for PE1000 and PE2000 although two separate curves are obtained. In striking contrast for PE3100 and PE4050 the data fall on sigmoidal curves as shown in Figure 12. Thus, for these fractions ΔH increases with T_c slowly at first, then at an accelerating rate, and finally at higher crystallization temperatures ΔH reaches a level where it increases more slowly with temperature. Since ΔH is proportional to the degree of crystallinity, which is very sensitive to morphological detail, it can reasonably be supposed that the sigmoidal curves reflect abrupt changes in the structure of interfacial regions of the crystals as the crystallization temperature increases.

The enthalpy of fusion data can be further examined in terms of the molecular nature of the crystals. The measured enthalpy of fusion ΔH is related to the surface enthalpy of the crystals q_e by an expression which can be derived from thermodynamic principles[21,22]

$$\Delta H = \Delta H_u - 2q_e/\xi \qquad (2)$$

where ΔH_u is the heat of fusion per segment for extended-chain crystals of infinite molecular weight, and ξ is the average number of segments in a section of the polymer chain running between the two lamellar surfaces and is equal to l/a, where l is the lamellar thickness and $a = 1.25$ Å is the projected length of the polyethylene monomer unit on the crystal c axis. Thus, a plot of ΔH against $1/l$ should be linear with an intercept equal to ΔH_u and a slope equal to $2aq_e$. Plots of the data according to eq 2 are shown in Figure 13 for the various fractions. It is seen that good linear relations are obtained for the fractions PE1000, PE2000, PE6750, and PE11600; the points for PE6750 and PE11600 fall on a single line, while PE1000 and PE2000 give a line with a different slope. On the other hand, for PE3100 and PE4050 the data points corresponding to higher values of $1/l$ coincide with the line for the two highest fractions, while the points corresponding to the lowest values of $1/l$ follow a different linear relationship with a slope intermediate between that of the highest and lowest fractions. For all the lines the intercept corresponding to $1/l = 0$ is 69.6 cal/g, which agrees well with the value of 68.6–70 cal/g expected for ΔH_u for polyethylene.[23,24] From the slopes of the plots, the values of the surface enthalpies q_e were calculated. Then combining these values with the known surface free energies σ_e, we calculated the values of the surface entropies s_e at $T = 400$ K in accordance with the well-known relation $\sigma_e = q_e - Ts_e$. The results are given in Table IV. It is interesting to compare the magnitudes of the observed surface enthalpies and entropies with values obtained by other investigators. For example, for solution-grown single crystals of a high

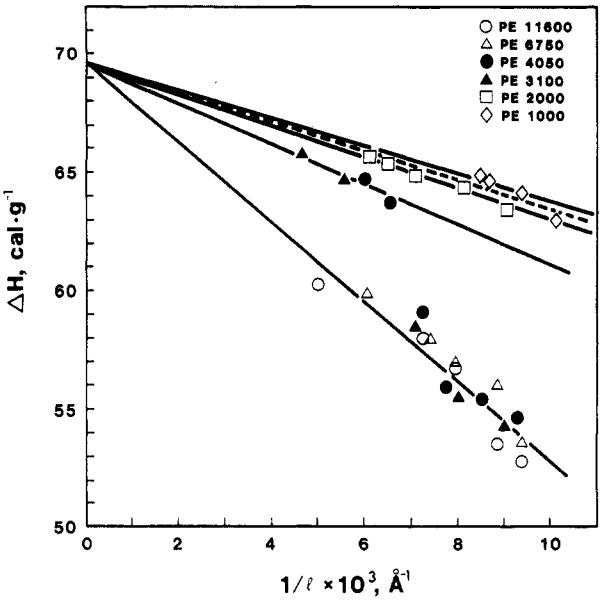

Figure 13. Plots of enthalpy of fusion ΔH as a function of reciprocal lamellar thickness for various polyethylene fractions crystallized from xylene. The slopes of the straight lines for PE1000 and PE2000 are so close to each other that within the experimental error, a common line can be drawn (broken line).

Table IV
Surface Enthalpy and Entropy of the Polyethylene Single Crystals

fraction	q_e,[a] kcal/(mol of folds)	s_e,[b] eu/(mol of segments)
PE11600	9.4	15.7
PE6750	9.4	16.8
PE4050 (high supercooling)	9.4	17.3
PE3100 (high supercooling)	9.4	17.3
PE4050 (low supercooling)	4.8	6.0
PE3100 (low supercooling)	4.8	6.5
PE2000	3.9	4.3
PE1000	3.4	5.7

[a] Surface enthalpy. [b] Surface entropy.

molecular weight polyethylene (Marlex 6000 Type 50) Roe and Bair[22] found $q_e = 22.1 \pm 2.0$ kcal/(mol of folds) and $s_e = 39 \pm 5$ eu/(mol of folds) at $T = 400$ K. The experimental values found for the present low molecular weight fractions are thus abnormally low, most probably because of chain-end effects.

In order to interpret these results in terms of the molecular nature of the crystals we must consider how the number of stems per molecule ν (i.e., the ratio of extended-chain length to lamellar thickness) varies with the temperature of crystallization for the various fractions. The relevant data are derived from measurements described in part 1. For crystals of PE2000, ν varies from about 1.6 to 1.0 over the accessible temperature range. Thus, the crystals of this fraction are essentially extended-chain structures. The surface free enthalpy of these crystals thus represents the enthalpy of a surface with only chain ends and cilia. Larger q_e values would suggest the existence of folds, chain ends, and possibly surface roughness.

As seen in Table IV, crystals of PE3100 and PE4050 grown in the high supercooling range (i.e., with larger values of $1/l$) have the same surface enthalpy as crystals of PE6750 and PE11600, which are at least twice folded over the range of crystallization temperatures studied. Lamellar thickness data for PE3100 and PE4050 crystals grown in this temperature range also indicate that the polymer chains are at least once folded. From these results

it is concluded that the structures of the interfacial regions of these crystals must be similar. The picture that emerges is that these crystals are composed principally of folded chains but because of the low values of σ_e and q_e they must also have a substantial number of chain ends in their interfacial regions.

For PE3100 and PE4050 the crystals grown at lower supercoolings (i.e., with lower values of $1/l$) have a surface enthalpy that is larger than that of extended-chain crystals but considerably lower than that of folded-chain crystals. This is consistent with the fact that in the corresponding temperature interval the values of ν (the number of stems per molecule) are in the range 1.5–2.2 for PE3100 and 2.3–3 for PE4050. The data thus suggest that the interfacial regions of these crystals contain both chain ends and folds, the former being in higher proportion. From these considerations it may be inferred that for the fractions PE3100 and PE4050 the sigmoidal shape of the ΔH vs. T_c plots indicates that there is an abrupt transition in the conformation of the molecules (i.e., in the number of folds per molecule) deposited on the growth faces of the crystals as T_c increases. As will be seen in part 3, evidence for such a transition is also obtained from growth rate data.

Conclusions

The magnitude of the basal surface free energy σ_e of polymer single crystals is an important indicator of the structure of the interfacial regions. The present work has shown that for low molecular weight solution-grown polyethylene single crystals the values of σ_e, obtained from plots of melting/dissolution temperatures against the reciprocal of the lamellar thickness, are in good agreement with those previously derived from an analysis of measurements of lamellar thickness as a function of undercooling. The values obtained increase with molecular weight and lie in the range of 40–60 erg/cm^2 for molecular weights from 3100 to 11600. By comparison with the value of about 93 erg/cm^2 expected for high molecular weight samples, which are essentially free of chain-end effects, the observed low values may be attributed to the presence of chain ends in the interfacial regions of the crystals.

Values of the equilibrium dissolution temperatures obtained from the intercept of the T_d vs. $1/l$ plots are in good agreement with those obtained from direct measurements on macroscopic extended-chain crystals of each fraction. These equilibrium dissolution temperatures correspond to the values for polymer chains of finite length and will be used subsequently in part 3 as the temperatures from which to measure the supercooling when analyzing kinetic data.

The enthalpies of fusion increase monotonically with crystallization temperature. This is to be expected from the previously observed increase of lamellar thickness with crystallization temperature for the same samples. Surprisingly, however, for the samples with molecular weights in the range of 3000–4000, the increase in the enthalpy of fusion follows a sigmoidal pattern. From this observation, in conjunction with surface enthalpy data, it is suggested that in this molecular weight range there is an abrupt transition in the structure of the interfacial regions of the crystals as the crystallization temperature increases. It is proposed that this change in interfacial structure involves a transition in the number of folds per molecule deposited on the growth faces as T_c increases. If this interpretation is correct, it is anticipated that evidence for such a transition should also be found in growth rate data. This will be discussed in part 3.

Acknowledgment. We thank Professors A. J. Kovacs, B. Wunderlich, and J. D. Hoffman for constructive discussions and critical comments on this work. We also gratefully acknowledge the support of the National Science and Engineering Research Council of Canada and the Ministère de l'éducation du Québec.

Registry No. PE (homopolymer), 9002-88-4.

References and Notes

(1) A. Keller, *Philos. Mag.*, **2**, 1171 (1957).
(2) E. W. Fischer, *Z. Naturforsch., A*, **12**, 753 (1957).
(3) J. P. Arlie, P. Spegt, and A. Skoulios, *Makromol. Chem.*, **99**, 160 (1966); **104**, 212 (1967).
(4) P. Spegt, *Makromol. Chem.*, **139**, 139 (1970); **140**, 167 (1970).
(5) A. J. Kovacs and A. Gonthier, *Kolloid Z. Z. Polym.*, **250**, 530 (1972).
(6) V. F. Holland and P. H. Lindenmayer, *J. Polym. Sci.*, **57**, 589 (1962).
(7) F. Hamada, B. Wunderlich, T. Sumida, S. Hayashi, and A. Nakajima, *J. Phys. Chem.*, **72**, 178 (1968).
(8) Manual for DSC-2C, Perkin-Elmer Corp., Norwalk, CT.
(9) M. J. O'Neill, *Anal. Chem.*, *36*, 1238 (1964).
(10) E. Hellmuth and B. Wunderlich, *J. Appl. Phys.*, **36**, 3039 (1965).
(11) A. J. Kovacs, A. Gonthier, and C. Straupe, *J. Polym. Sci., Part C*, **50**, 283 (1975).
(12) B. Wunderlich, *Polymer*, **5**, 611 (1964).
(13) D. A. Blackadder and H. M. Schleinitz, *Polymer*, **7**, 603 (1966).
(14) J. D. Hoffman and J. J. Weeks, *J. Res. Natl. Bur. Stand., Sect. A*, **66**, 13 (1962).
(15) T. W. Huseby and H. E. Bair, *J. Appl. Phys.*, **39**, 4969 (1968).
(16) H. E. Bair, T. W. Huseby, and R. Salovey, *Polym. Prepr., Am. Chem. Soc., Div. Polym. Chem.*, **9**, 795 (1968).
(17) H. E. Bair and R. Salovey, *J. Macromol. Sci., Phys.*, **B3**, 3 (1969).
(18) J. D. Hoffman, L. J. Frolen, G. S. Ross, and J. I. Lauritzen, Jr., *J. Res. Natl. Bur. Stand., Sect. A*, **79**, 671 (1975).
(19) L. Mandelkern, J. M. Price, M. Gopalan, and J. G. Fatou, *J. Polym. Sci., Part A-2*, **4**, 385 (1966).
(20) C. P. Buckley and A. J. Kovacs, *Colloid Polym. Sci.*, *254*, 695 (1976).
(21) L. Mandelkern, A. L. Allou, Jr., and M. Gopalan, *J. Phys. Chem.*, **72**, 309 (1968).
(22) Ryong-Joon Roe and H. E. Bair, *Macromolecules*, **3**, 454 (1970).
(23) L. Mandelkern, *Rubber Chem. Technol.*, **32**, 1392 (1959).
(24) B. Wunderlich and C. M. Cormier, *J. Polym. Sci., Polym. Phys. Ed.*, **5**, 987 (1967).